

EMC3-Eirene/SOLPS4.3 comparison for ITER

Y. Feng¹⁾, T. Lunt¹⁾, A. Kukushkin²⁾, M. Becoulet³⁾, T. Casper²⁾, T. Evans⁴⁾,

H. Frerichs⁵⁾, A. Loarte²⁾, R. A. Pitts²⁾, D. Reiter⁵⁾, O. Schmitz⁵⁾

1) *Max-Planck-Institute fuer Plasmaphysik, Greifswald/Garching Germany*

2) *ITER Organization, Route de Vinon sur Verdon, 13115 St Paul Lez Durance, France*

3) *CEA/IRFM, Cadarache, 13108 St Paul-lez-Durance Cedex – France*

4) *General Atomics, P.O. Box 85608, San Diego, California, 92186-5608 USA*

5) *Institute for Energy Research-Plasma Physics, Forschungszentrum Jülich, Germany*

1. Introduction

The 3D scrape-off layer (SOL)-plasma transport code EMC3-Eirene [1, 2] is being employed to evaluate the non-axisymmetric heat and particle flows induced by the ELM-controlling RMP fields foreseen for ITER [3]. The work began with a benchmark against the SOLPS4.3 (B2-Eirene) code [4] – the major numeric tool used to assess the ITER divertor performance in the axisymmetric case. The benchmark aims at checking the compatibility in the most relevant physics assumptions between the two codes, in particular under low divertor temperature conditions of interest. Similar benchmarks against other 2D models have been made for AUG [5] and JET [6], nevertheless without impurities. This paper presents the benchmark process at ITER and the results obtained, with emphasis on the cases with impurities. Two different models for dealing with the impurity radiation in EMC3: the intrinsic impurity transport model and a “coronal”-equilibrium model, are presented and compared.

2. Major differences in geometry and physics assumptions between the two codes

The two codes were run in their respective forms as they are. The major differences in geometry and physics setup relevant to this benchmark are listed in table 1.

Table 1: Major differences in geometry and physics between the two codes

	SOLPS4.3	EMC3-EIRENE
Geometry	Flux-surface-based 2D grid, strictly axisymmetric	Field-line-aligned helical 3D grid, approximation of the axisymmetry
Physics	multi-fluid of various ion species, flux limit for parallel transport, more comprehensive set of atomic reactions & ion species	hydrogen isotope with “trace”-impurities, parallel transport purely classical, volume recombination not yet included
Boundary Conditions	$M_{\text{targ}} \geq 1$ $\gamma_e, \gamma_i = \text{functions of } n_e, T_e, T_i$	$M_{\text{targ}} = 1$ $\gamma_e=4.5, \gamma_i = 2.5$ (for the internal energy flow)

3. Inputs and boundary conditions

The benchmark is performed for an axisymmetric H-mode configuration with $I_p=15\text{MA}$. Deuterium plasma is assumed. A spatially-constant diffusivity $D = 0.3 \text{ m}^2/\text{s}$ is set equal for all ion species and an anomalous heat conductivity of $1 \text{ m}^2/\text{s}$ is assumed for both electrons and ions. The perpendicular viscosity is set to be $0.2\text{m}^2/\text{s}$ in SOLPS4.3, while it is fixed to equal D in the EMC3 code. A 3cm decay length is set at the outer boundary for density and temperatures. At the inner boundary, EMC3 aligns the density at the outer midplane with that of SOLPS4.3. The power entering the SOL, P_{SOL} , is split equally between electrons and ions.

4. Main results

4.1 Without impurities

The first comparison is made for a pure deuterium plasma with external particle fluxes of $9.1 \cdot 10^{21} \text{ s}^{-1}$ across the innermost boundary surface and $2.25 \cdot 10^{22} \text{ s}^{-1}$ via gas-puffing from an upper port. P_{SOL} is set to be 60 MW. In the SOLPS4.3 calculations the external particles are

pumped out by defining a finite absorbing surface underneath the divertor dome. In the EMC3-Eirene simulations the two external particle sources are sequentially switched on and the global particle balance is kept by uniformly reducing an “effective” recycling coefficient at the targets. Figure 1 compares the respective T_e , T_i , n_e and $(T_e+T_i) \cdot n_e$ profiles at the outer midplane. Excellent agreement is found for all the profiles. The gas-puff ($\sim 0.6\%$ of the recycling flux) makes effects visible only in the far SOL T_i and n_e and the external particle core flux ($\sim 0.25\%$ of the recycling flux) is too small to be reflected in the upstream profiles.

The target plasma profiles are compared in figure 2. The power load profiles agree well in form and level on both the inner and outer targets, while certain discrepancies exist in the T_e and n_e profiles. Different sets of the energy sheath transmission factors assumed in the two codes are the most possible contributors to these discrepancies. Note the highly-sensitive state of the downstream plasma in the high-recycling regime.

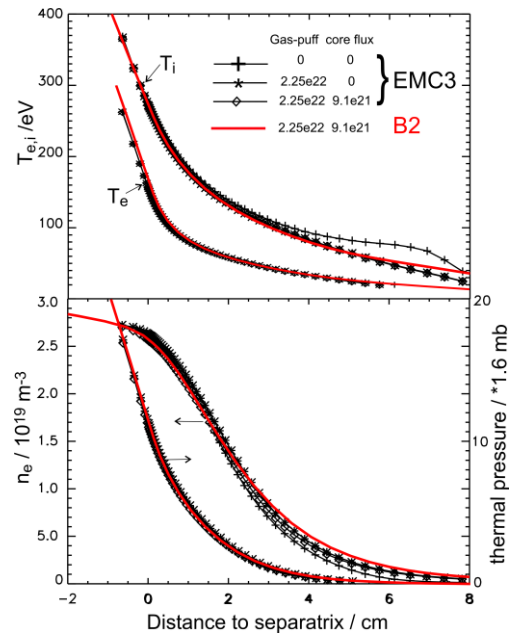


Fig.1: Excellent agreement in upstream plasma profiles

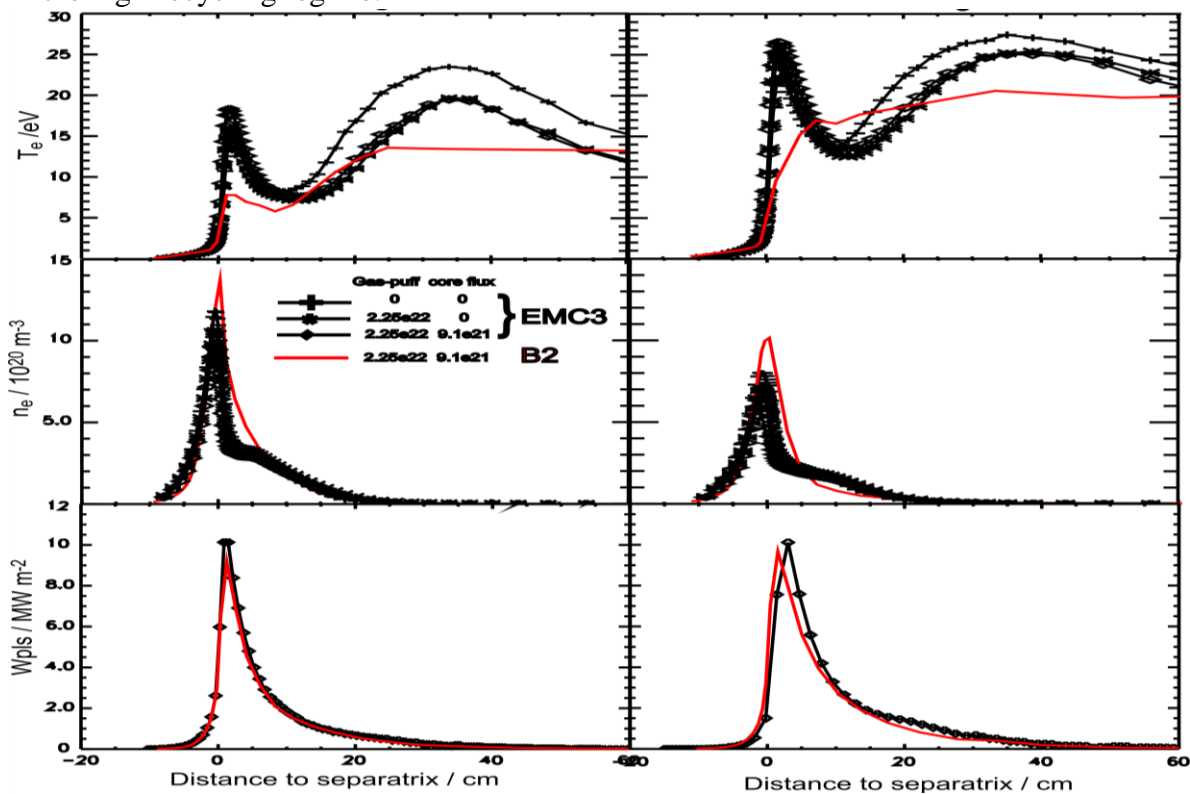


Fig.2: Comparison of plasma profiles at the inner (left) and outer (right) target. From top bottom: electron temperature and density and the power load from charged particles.

4.2 With impurities

The next comparison is made for a case where $\sim 40\%$ of a 50 MW input power is removed by the impurity line radiation. While SOLPS4.3 includes carbon and helium as separate fluid species, EMC3 takes only the carbon radiation into account which is treated by two different

models for comparison: the intrinsic impurity transport model adopted in EMC3 and a “coronal”-equilibrium model. The resulting power deposition profiles are compared in figure 3. In comparison to the 2D code, the 3D code predicts somewhat broader power load profiles on both the inner and outer targets. The assumption of “coronal”-equilibrium slightly underestimates the peak value of the power load on the outer target. The plasma thermal pressure profiles (not shown here) agree very well between the two codes on both targets. However, discrepancies in the resolved n_e and T_e profiles are apparent (figure 4), even within the same 3D code between the two different radiation models (see the profiles on the outer target). In view of the low T_e around the strike-point, any differences in details of the radiation distribution are expected to have strong impacts on the n_e and T_e profiles there.

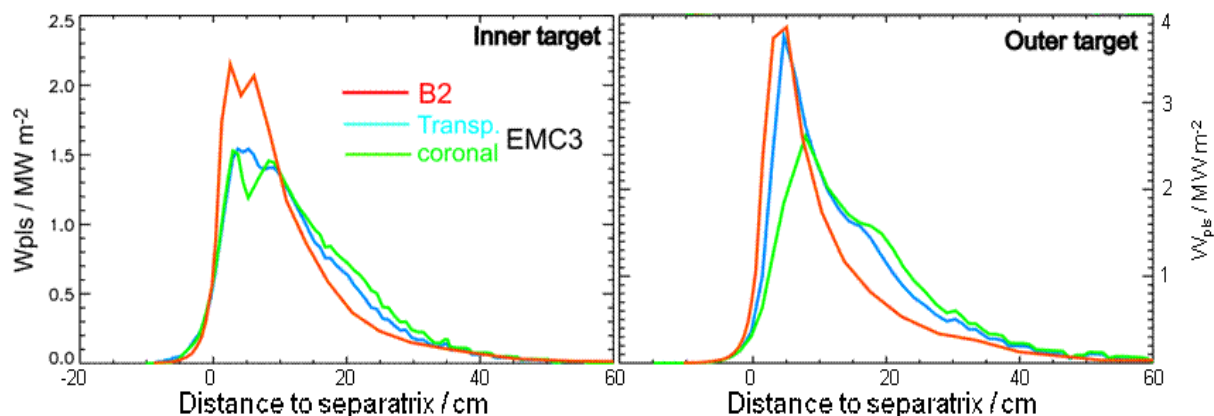


Fig.3: Comparison of power load distributions predicted by the two codes.

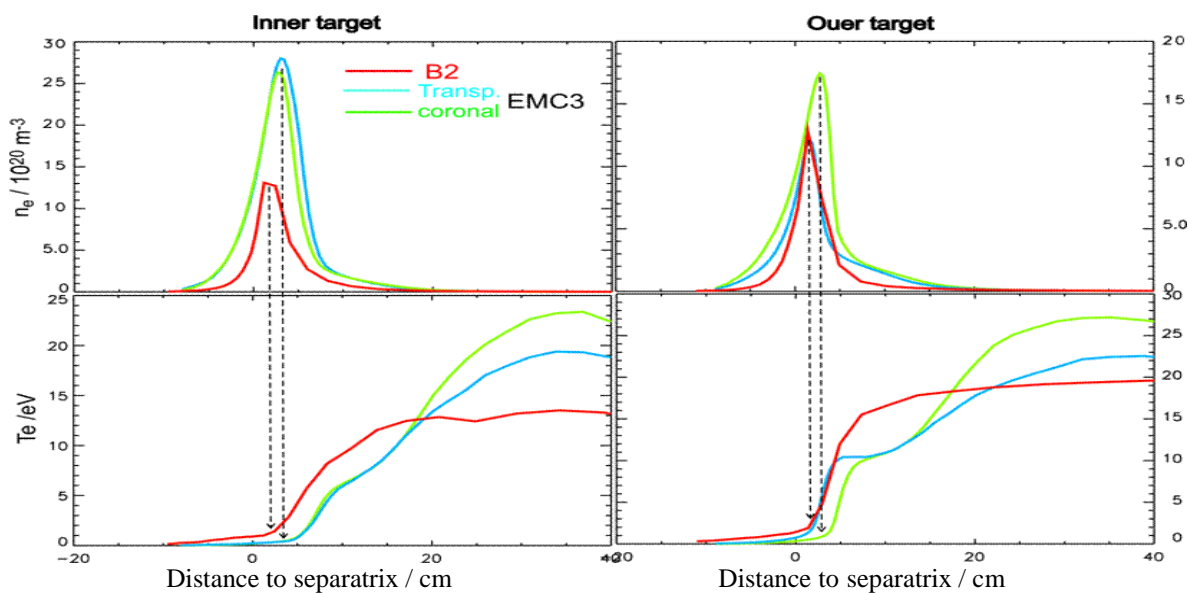


Fig. 4: Comparison of n_e and T_e profiles downstream

Applying the intrinsic impurity transport model of EMC3, helical mode-like structures are observed at the colder inner divertor leg when the radiation fraction increases above $\sim 20\%$ (s. figure 5). As already pointed out in section 2, the field-line-aligned 3D grid of finite resolution does not preserve the toroidal symmetry of the poloidal divertor perfectly. The axisymmetry condition is not imposed in the 3D modelling, neither implicitly nor explicitly. An axisymmetric imperfection of the 3D grid is the most likely reason for the emergence of spurious 3D effects in SOL plasmas of a highly-sensitive state close to detachment. To clarify how fine the 3D grid must be in order to remove the finite grid resolution effects is interesting, nevertheless, less relevant to the 3D applications specified within the ITER task due to the already-considerable computational effort involved. This will be continued in an independent

activity. Instead, an effective radiation model based on “corona”-equilibrium is tested and compared with the transport model (figures 4 and 5). No helical effects are identified in the “corona”-equilibrium model results up to a radiation level of 40% of P_{SOL} and the two radiation models result in similar radiation patterns and plasma profiles downstream, except for the much thinner radiation bands produced by the “corona”-equilibrium model because of the absence of carbon transport.

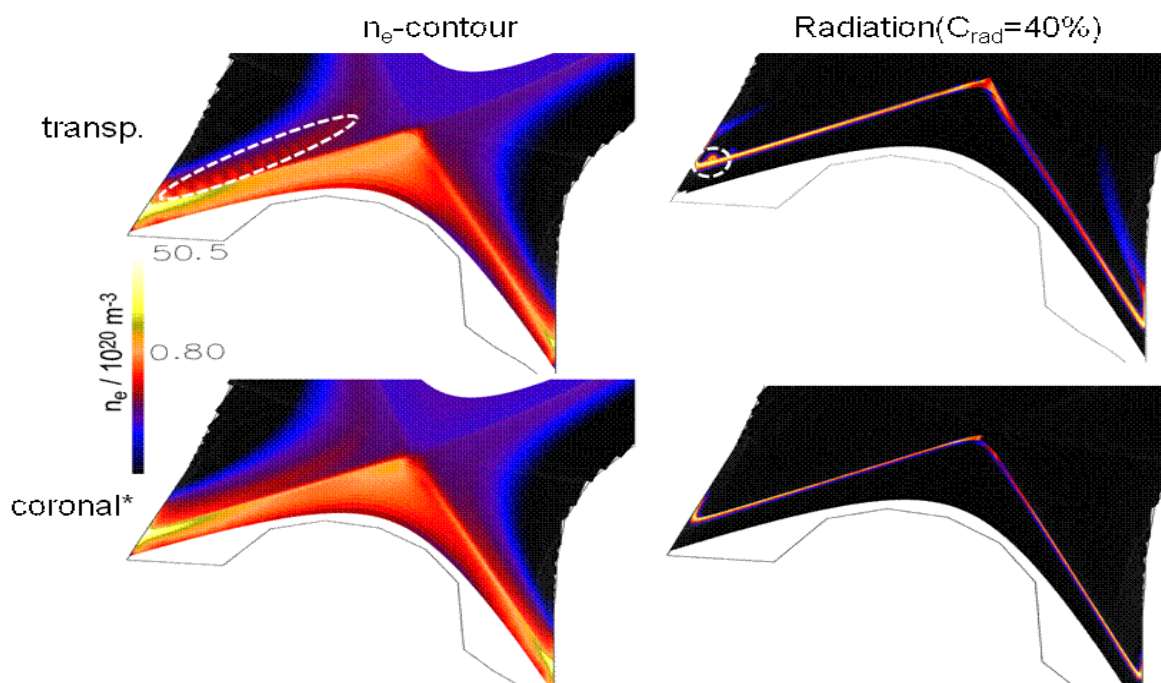


Fig.5: Transport and “coronal”-equilibrium models result in similar electron density contours and radiation patterns except for the disappearance of the helical effects in the latter case.

5. Conclusion

SOLPS4.3 and EMC3-Eirene are compared for an axisymmetric ITER divertor configuration (15MA H-mode) under various SOL-plasma conditions for cases with and without impurities. In the absence of impurities, the two codes predict almost the same upstream plasma profiles and the same heat flux distributions on both the inner and outer targets. Switching on impurities causes slight deviations in these profiles and certain discrepancies in profile details of the downstream temperatures and density between the two codes have been observed in all the cases used for the comparison. These discrepancies are consequences of the differences in the physics models adopted in the two codes and are regarded as being well within the range acceptable for this benchmark. An effective radiation model based on “coronal” equilibrium results in reasonable power flux distributions on targets. This model has been tested for a radiation fraction up to 40%.

References

- [1] Feng Y. *et al.* 2004 *Contrib. Plasma. Phys.* **44** 57
- [2] Reiter D. *et al.* 2005 *Fusion Science and Technology* **47** 172
- [3] Schmitz O. *et al.*, Fusion for Energy grant F4E-GRT055 (PMS-PE) “Study of power and particle fluxes to plasma-facing components during ELM control by in-vessel coils in ITER and evaluation of plasma response effects”
- [4] Kukushkin A.S. *et al.* 2008 Proc. 35th EPS Conf. on Controlled Fusion and Plasma Physics (Hersonissos, Greece, 2008), paper P1-013
- [5] Lunt T. *et al.* 2009 36th EPS Conference on Plasma Phys. Sofia, June 29 - July 3, 2009 ECA Vol.33E, P-1.154
- [6] Harting D. *et al.* 2011 to be published in J. Nucl. Mater.